Journal of Power Sources 247 (2014) 786–793

Contents lists available at ScienceDirect

Journal of Power Sources

journal homepage: www.elsevier.com/locate/jpowsour

Sequential effect and enhanced conductivity of star-shaped diblock liquid-crystalline copolymers for solid electrolytes

Yongfen Tong [a, b], Lie Chen [a], Xiaohui He [a], Yiwang Chen [a, *]

[a] Institute of Polymers, Department of Chemistry, Nanchang University, 999 Xuefu Avenue, Nanchang 330031, China
[b] School of Environmental and Chemical Engineering, Nanchang Hangkong University, 696 Fenghe South Avenue, Nanchang 330063, China

HIGHLIGHTS

- Novel star-shaped amphiphilic liquid crystalline copolymers are prepared.
- The copolymers consist of mesogenic segment and hydrophilic poly(-ethyleneoxide)s.
- Lamellar structures are achieved by cooperative assembly.
- The ionic channel is aligned greatly by orientation of the mesogens.
- Consequently ionic conductivity is improved.

GRAPHICAL ABSTRACT

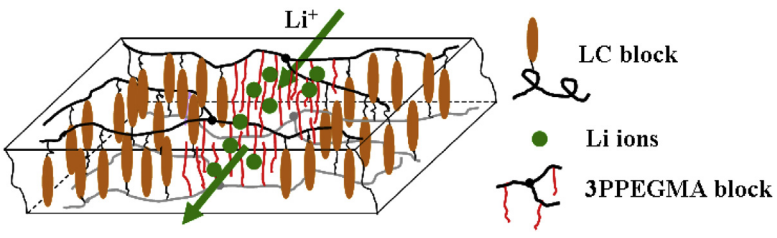

ARTICLE INFO

Article history:
Received 18 June 2013
Received in revised form
30 August 2013
Accepted 31 August 2013
Available online 20 September 2013

Keywords:
Polymer electrolytes
Star-polymers
Liquid crystals
Ionic conductivity

ABSTRACT

Star-shaped polymers are synthesized by atom transfer radical polymerization using poly-(methoxy-poly (ethylene glycol) methacrylate) (PPEGMA) as a hydrophilic segment and poly {10-[(4-cyano-4′-biphenyl) oxy] decatyl methacrylate} (PMALC) as a hydrophobic liquid crystalline segment. Lamellar morphology is also achieved by cooperative assembly of hydrophobic mesogen-containing polymethacrylates and the amorphous hydrophilic PPEGMA nanoscale aggregation, especially after liquid crystal thermal annealing. In addition, the sequential effect, that is, the position difference of the liquid crystalline segments in the copolymer electrolytes causes two quite different morphologies. The liquid crystalline segments arranged in the star polymer inner sphere makes it difficult for the mesogens to interact with each other efficiently, which leads to a discontinuous molecular packing. However highly ordered domains can be formed in the electrolytes with mesogens in the star copolymer exterior, which can provide a more favorable morphology for the ions transportation. As a result, incorporation of the liquid crystalline segments into the copolymer has improved ionic conductivity of electrolytes, especially for the 3PPEGMA-PMALC with the mesogen arranged in the outside of star copolymer sphere. Ionic conductivity of 3PPEGMA-PMALC annealed at liquid crystalline state is 1.0×10^{-4} S cm^{-1} at 25 °C, which is higher than that of 3PPEGMA electrolytes without mesogen groups.

1. Introduction

Solid polymer electrolyte (SPE) has been extensively studied for more than 20 years as an alternative for the traditional liquid electrolyte in lithium-ion cells because of their potential applications in many solid electrochemical devices such as high-energy density batteries, electrochromatic windows, chemical sensors, and light-emitting devices. [1,2] Most of the research work focused on poly (ethylene oxide) (PEO) and its derivatives as a polymer matrix, due to the ability of PEO to dissolve salts and high segmental flexibility for ion transport in the amorphous phase [3,4]. However, linear PEO-based polymer electrolytes show

* Corresponding author. Tel.: +86 791 83969562; fax: +86 791 83969561.
E-mail address: ywchen@ncu.edu.cn (Y. Chen).

0378-7753/$ – see front matter © 2013 Elsevier B.V. All rights reserved.
http://dx.doi.org/10.1016/j.jpowsour.2013.08.139

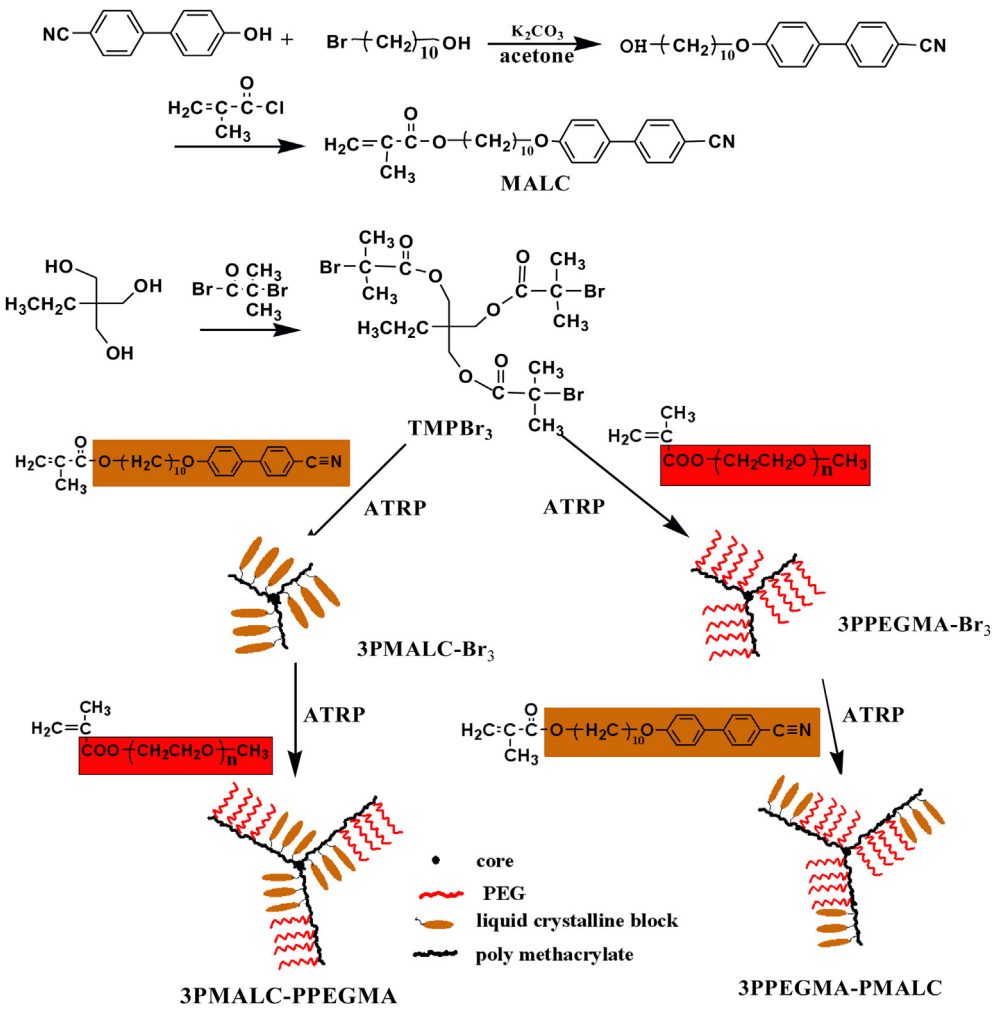

Scheme 1. Synthesis routes for monomers and copolymers.

comparatively low ionic conductivity ($\sim 10^{-7}$ S cm^{-1}) at ambient temperature. The inherent limitation of ion transport in a solid PEO-based electrolyte system makes it unlikely to reach the level of ionic conductivity for practical applications, because an ionic conductivity of 10^{-3} S cm^{-1} at room temperature is generally required for an energy storage device. Several research groups reported that the graft polymer electrolytes with more flexible oligomeric PEO side chains exhibited the higher ion conductivities (10^{-5}–10^{-6} S cm^{-1}) at ambient temperature [5,6]. Higa et al. [7] synthesized a graft copolymer electrolyte which contained a polyimide main chain and methoxy-poly (ethylene glycol) methacrylate side chains, showing a relatively high conductivity (6.5×10^{-6} S cm^{-1} at 25 °C) and excellent tensile strength (100 MPa). Zuo et al. [8] prepared a novel graft copolymer solid electrolyte, where methacrylate backbone is attached with (C_{16})-methoxyl terminated oligo(ethylene oxide) side chains, exhibited the ionic conductivity value of $\sim 1.3 \times 10^{-4}$ S cm^{-1} at 30 °C and 7.9×10^{-4} S cm^{-1} at 80 °C. Another favorable solution to this problem involves the use of molecular assembly of block copolymers, and much research effort focused on the production of novel block copolymers bearing liquid crystalline (LC) or hydrophobic blocks because of their fascinating ordered phenomena [9]. These block copolymers have the advantage of combining the properties of liquid crystals and block copolymers; which provides not only novel functionality but also the possibility of microphase separation formation due to the regular ordering of the liquid crystals. A variety of electrolytes with enhanced performance based on LC block copolymers have been reported [10–15].

Star-shaped polymers are a class of branched polymers having a globular architecture, which are expected to exhibit unique physical properties and morphologies not observed in the corresponding linear polymers. [16,17] In particular, the crystallinity and degree of chain entanglement of star-shaped polymers are smaller than those of the linear polymers [18]. Niitani et al. described the application of star-shaped polystyrene-*b*-poly((polyethylene glycol) methyl ether methacrylate) for SPE, finding that the star-shaped block polymer electrolytes exhibited the enhanced lithium battery performances [19]. Kim et al. also studied the star-shaped polymer electrolytes with POSS and PEG side groups for SPEs, yielding an ionic conductivities of 1.75×10^{-5} S cm^{-1} at 30 °C, which is two orders of magnitude higher than that of the star-shaped polymer electrolyte with MMA moiety [20].

In this study, we designed star-shaped polymers containing poly-(methoxy-poly (ethylene glycol) methacrylate) (PPEGMA) as a hydrophilic segment and poly {10-[(4-cyano-4′-biphenyl) oxy] decatyl methacrylate} (PMALC) as a hydrophobic liquid crystalline segment by atom transfer radical polymerization (ATRP) [21–23]. The novel star copolymer electrolytes, where a PMALC segment is responsible for orientation and a PPEGMA segment is used as lithium-ion conduction pathway, are expected to present the

enhanced ion conductivity via ion hopping along the amorphous branched structure in an ordered morphology, resulting from the cooperative assembly of mesogenic pendants and flexible segments. Two copolymer electrolytes, 3PMALC-PPEGMA and 3PPEGMA-PMALC with the PMALC segment at different position (interior or exterior) have been designed and synthesized. Scheme 1 shows the synthesis routes for monomers and copolymers. The liquid crystalline properties, thermal properties, morphology and ionic conductivity of the star copolymer electrolytes have been studied and the influence of the sequential effect on their properties has also been investigated.

2. Results and discussion

2.1. Structural characterization of polymers and electrolytes

The synthesis and structure of the monomers and copolymers are outlined in Scheme 1. All the reactions and manipulations are carried out under a nitrogen atmosphere. The copolymers were synthesized by ATRP and the synthesis details have been elaborated in Supporting information. The excess of 2-bromoisobutyryl bromide was used to react with trimethylolpropane, which ensured the completely consumption of −OH in starting materials to afford 3-arm structure. Star polymers prepared from each macroinitiator were characterized via gel permeation chromatography (GPC), FT-IR (see Supporting Information, Fig. S1) and ^{1}H NMR analysis. Compared with that of the related star precursor in Fig. 1, the GPC curves of corresponding copolymers shift to the higher molecular weight region suggesting that block copolymers have been synthesized successfully. Low polydispersity (PDI < 1.40) is observed for all the copolymers prepared indicating the controlled polymeric architecture with narrow molecular weight distribution was generated in all cases. The star shaped structure can be confirmed by the disappearance resonance peak of −OH of starting materials in ^{1}H NMR of resulting polymers (See Supporting information). The ^{1}H NMR spectra of the star-shaped polymers 3PPEGMA-PMALC and 3PMALC-PPEGMA in deuterated chloroform are shown in Fig. 2, and those of the intermediates have also been given for comparison. Obviously, the well-specified molecular structure of 3PPEGMA-PMALC and 3PMALC-PPEGMA can be well assigned in the NMR spectra. The resonance peaks at 0.8–2 ppm are associated

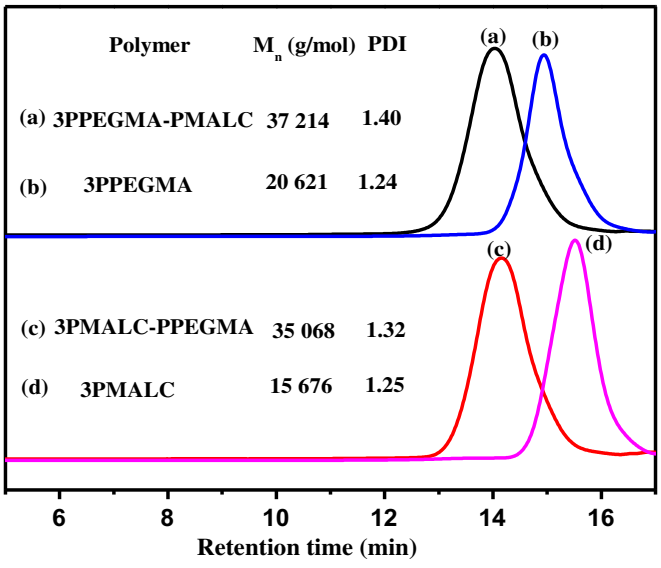

Fig. 1. GPC curves of 3PMALC, 3PPEGMA, 3PMALC-PPEGMA, and 3PPEGMA-PMALC, respectively.

to the protons from the methacrylate backbone. The proton peaks from PEG side chains (δ = 3.5–4.1 ppm, CH_2–CH_2–O and 3.41 ppm, CH_3–O) indicate the inclusion of PEGMA in the 3PPEGMA, 3PPEGMA-PMALC and 3PMALC-PPEGMA polymers. Proton peaks observed at δ = 6.9–7.6 ppm are clearly assigned to the phenyl proton of the LC groups. Therefore, ^{1}H NMR analysis supports the successful synthesis of the star copolymers containing mesogens.

The absorption spectra of the spin-coated films of the copolymers are given in Fig. S2. The UV–vis maximum absorption peak of the as-prepared films at 293 nm decreased greatly after annealing, probably attributed to the out-of-plane alignment of the cyanobiphenyl mesogens, which is similar to literature reported results [24,25]. Moreover, a red shift of about 5 nm appeared after annealing, due to the more oriented π–π stacking [26].

The interaction between the polar groups and Li^+ ions in the electrolytes has been characterized by IR spectra. Generally, the carbonyl (C=O) and ether (C–O–C) groups bonded with Li^+ always results in the related absorption peaks shifting to the lower wave number because of the reduced electron density [27,28]. The phenomenon also can be observed in the IR spectra of several 3PPEGMA-PMALC based electrolytes, presented in Fig. S3. The ether bond absorption peak of 3PPEGMA-PMALC based electrolytes shifts to the lower frequency as the increase of the salt concentration. The peak at 1727 cm^{-1} assigned to the carbonyl group of the methacrylate does not change with the lithium salt concentration. The reason is that there is a competition between C=O groups and C–O–C groups to coordinate with Li^+. Most of the Li^+ ions tend to coordinate to the ether bond since the content of C–O–C groups in the studied electrolytes is much higher than that of C=O groups [8].

2.2. Thermal behaviors and liquid crystallinity

Temperature for 5 wt% loss has often been used as a degradation temperature (T_d) to estimate thermal stability of a synthetic polymer. The T_d values for 3PPEGMA, 3PPEGMA-PMALC and 3PMALC-PPEGMA are approximately 290 °C (see Fig. 3), indicating that the 3-arm copolymers are thermally stable. Fig. 4 shows microphotographs of the mesomorphic textures of monomer MALC, 3PMALC, copolymers 3PMALC-PPEGMA, 3PPEGMA-PMALC and corresponding electrolytes doped with the lithium salt taken under a polarized optical microscope (POM). From the figure we can see that monomers and copolymers exhibit the enantiotropic liquid crystallinity. The cyanobiphenyl mesogen possesses so strong self-assembly ability that all of copolymers present optical anisotropy with birefringent textures when heated or cooled even after doped with $LiClO_4$. The mesomorphic behavior of copolymers and electrolytes also has been studied by differential scanning calorimetry (DSC) and the samples are first heated to 180 °C to remove thermal history. The DSC traces of the star copolymers display rich phase transitions, as shown in Fig. 5A. In the subsequent first cooling cycle, the isotropic to liquid-crystalline (LC) transition is observed at 96.0 °C for 3PPEGMA-PMALC and 91.4 °C for 3PMALC-PPEGMA, and the exothermic peak is ascribed to the linear block PEG crystallization upon cooling between 6.8 and 14 °C. In the second heating cycle, transition temperatures (T_i) from the LC to isotropic are located between 96 and 103 °C, and the glass transitions of PEG block in 3PPEGMA-PMALC and 3PMALC-PPEGMA are observed at −60.1 and −51.8 °C, respectively. 3PEGMA-PMALC electrolytes show obvious endothermic peak in the DSC curve at about 102 °C (shown in Fig. 5B), indicating that the electrolytes are liquid crystals. The Tg of the copolymer increases with the salt concentration increasing, which can be attributed to ion–dipole interactions reducing the segmental motion of the copolymer electrolytes [29]. The transition temperatures and the enthalpies of the star

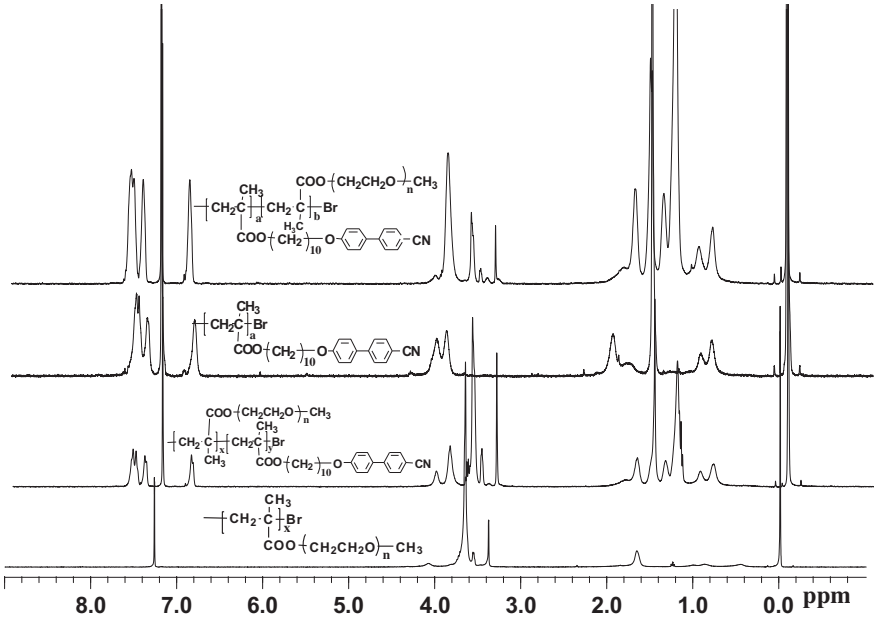

Fig. 2. ^{1}H NMR spectra of the copolymers 3PPEGMA, 3PPEGMA-PMALC, 3PMALC, and 3PMALC-PPEGMA.

copolymers and electrolytes with various [O]/[Li^+] ratios have been recorded and summarized in Table S1. 3PPEGMA shows the lowest Tg and 3PMALC-PEGMA has the highest Tg for the reason of the filler effect of LC contents. Interestingly, the copolymers of 3PPEGMA-PMALC and 3PMALC-PPEGMA have almost the same content of rigid LC moieties and only differ with sequence of PEGMA and PMALC blocks, but the Tg of 3PPEGMA-PMALC is still lower than that of 3PMALC-PPEGMA. This implies that the rigidity of LC moieties in the exterior of the star copolymer can reduce the increase of Tg through increasing the free volume and external plasticization [30].

2.3. Morphology of the copolymers and electrolytes

The microstructures of the star copolymers and electrolyte films were studied using X-ray diffraction, and the films annealed at their liquid crystalline states are added for comparison (Fig. 6). Compared to the as-cast film, the XRD diffractogram of all the films

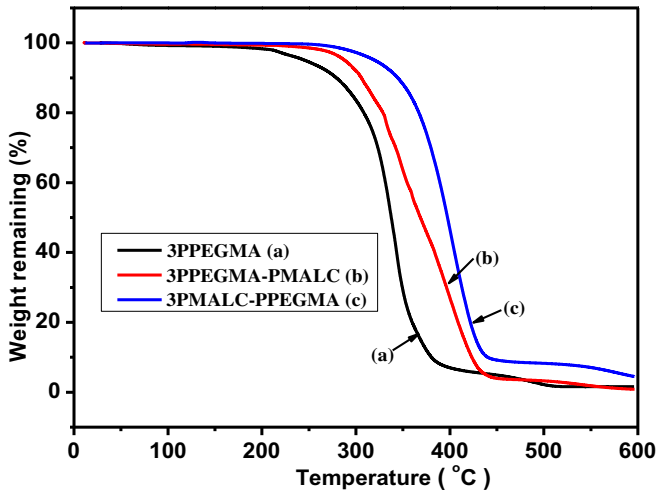

Fig. 3. TGA thermogram of 3-arm polymers recorded under nitrogen at a heating rate of 10 °C min^{-1}.

annealed at the liquid crystalline state show an obvious reflection at $2\theta = 5.6°$, corresponding to a layer spacing of 15.80 Å (d_1), which is close to the molecular length of side chain with mesogens. The peak located at $2\theta = 3.9°$ ($d_2 = 22.67$ Å) is associated to the methylene chain distance of the side chain, that is, the distance between the mesogenic to backbone. The mesophase of the copolymer thus may consist of such a layered structure as shown in Fig. 7. It suggests that the formation of liquid-crystalline domains with well-ordered crystalline nanostructure can be induced by oriented cyanobiphenyl after LC thermal annealing [31]. We also carried out powder X-ray diffraction (XRD) experiments on the copolymers at different temperature with the aim to collect more information on the mesomorphic structure (Fig. S4). Upon heating, no apparent variation in the WAXD profile is seen until the temperature reaches to 90 °C, where a diffraction hump at $2\theta = 2.2°$ has emerged for 3PPEGMA-PMALC copolymer (Fig. S4A). Further heating up to 100 °C results in the reflection peaks sharpened and reaching their maximum intensities. The sharp reflection at $2\theta = 2.2°$ with a layer spacing of $d_3 = 39.53$ Å is corresponding to the interdigitated manner of the repeat unit of liquid-crystalline side chains in its most extended conformation. The mesogens arranged in an antiparallel overlapping interdigitated manner of the structure is schematically shown in Fig. 7. At 110 °C, the reflections disappeared, indicating that the spontaneous assembly of the liquid-crystalline molecules pushes star copolymers to form oriented structure upon heating at liquid-crystalline states. In contrast to the 3PPEGMA-PMALC, the XRD diffractograms at different temperature of the 3PMALC-PPEGMA show more diffuse around $2\theta = 2.2°$. This suggests that the sequence of the mosogens and PEGMA is crucial for the molecular packing, and the mesogens arranged in the outside of the copolymer is more favorable. The packing arrangement of molecules also can be supported by AFM and TEM analysis (discussed later).

We investigated the surface structure of the copolymer films by using an atomic force microscope (AFM). As shown in Fig. S5a and S5b, novel wormlike microphase domains are clearly observed in AFM images of annealed 3PPEGMA-PMALC films due to the difference in elastic modulus between amorphous PPEGMA and cyanobiphenyl phases, which is different from the phase segregated

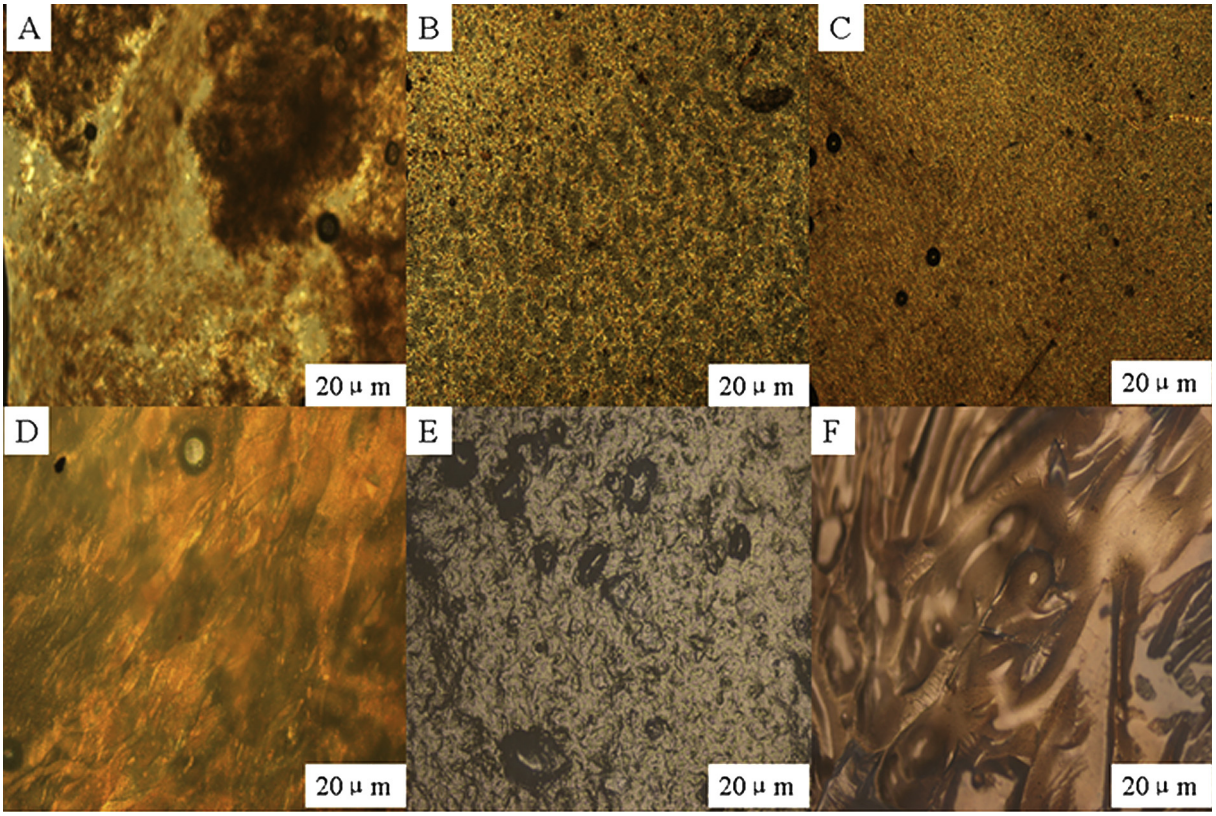

Fig. 4. Mesomorphic textures observed on cooling (A) MALC, (B) 3PMALC, (C) 3PMALC-PPEGMA, (D) 3PPEGMA-PMALC, and electrolytes ([O]/[Li^+] ratios = 20) (E) 3PMALC-PPEGMA, (F) 3PPEGMA-PMALC from their isotropic melts, respectively.

morphologies of block copolymers with weak molecular interactions [32]. The structure of 3PMALC-PPEGMA has been manifested by the distinctive aggregated morphology, as shown in Fig. S5c and S5d. Discontinuities of the cylindrical packing are caused by the LC mesogens in the star polymer inner sphere, which makes it difficult for the mesogens to interact with each other efficiently.

Transmission electron microscopy (TEM) was further employed to supplement the AFM findings and explore the morphology of the star copolymers. Two typical TEM images are shown in Fig. 8. The copolymers exhibit well-defined morphologies with the nano-scale microphase-separation between the mesogen functionalized hydrophobic block and the hydrophilic PPEGMA block. The flexible PPEGMA blocks show more dark domains compared with the cyanobiphenyl mesogenic blocks with the lighter regions. [33] A typical striped morphology of 3PPEGMA-PMALC copolymer in their LC state (Fig. 8a) proves the formation of highly ordered domains with a lamellar structure, in a good agreement with those from AFM measurement. Fig. 8b shows an irregular phase separation for 3PMALC-PPEGMA at 95 °C. The discontinuities of the triangulate stripes, marked by ellipses, should be related to the 3-arm LC segment in inner sphere. The two entirely different morphologies demonstrate the sequential effect of the same component star copolymers. Computer-generated molecular geometry of 3PPEGMA-PMALC shows a better interaction for the molecular than that of 3PMALC-PPEGMA in Fig. S6.

From the combination of all investigation results, a model for the self-assembled structure of star shape liquid crystalline copolymer is proposed as schematically sketched in Fig. 9, where the amorphous PPEGMA nanoscale aggregation is orientated by LC groups and the whole composite, and the ion-conducting layer of the ethylene oxide part as a hydrophilic segment and the layer of aromatic parts as hydrophobic liquid crystalline segments afford an ordered ion mobility pathway.

2.4. Ionic conductivity

Fig. 10 plots the dependence of the conductivity on 1/T for all three copolymer electrolytes in the temperature range from 25 °C to 85 °C. The ionic conductivity increases with the elevated temperature, although their profiles are somewhat different from each other. The ionic conductivity of the copolymer electrolytes based on 3PPEGMA-PMALC and 3PMALC-PPEGMA with mesogen segment are lower than that of 3PPEGMA electrolyte at low temperature, probably because the LC groups cannot transfer the lithium ions effectively. However with temperature increasing, the ionic conductivity value of the liquid crystalline copolymer is higher than that of 3PPEGMA electrolyte. The improved ionic conductivity suggests that orientation of mesogens favors the formation the conducting pathway with less entanglement and promotes more cooperative motion of the grafted PEG side chains [34]. The sequence of the segments in the star copolymers also has some influence on the conductivity because 3PPEGMA-PMALC developed more ordered morphology than its analogous copolymer 3PMALC-PEGMA. Comparing 3PPEGMA-PMALC with 3PMALC-PEGMA, the former has relatively higher conductivity values throughout all the temperature. Moreover, the glass transition of the PEG moiety for the 3PPEGMA-PMALC and 3PMALC-PPEGMA electrolytes is observed at −60.1 °C and −51.8 °C respectively. This observation suggests that the PEG moiety of the 3PPEGMA-PMALC electrolytes shows higher mobile at room temperature, more beneficial for Li-ions transportation.

Fig. 11 shows the temperature dependence of the conductivity for 3PPEGMA-PMALC electrolyte with various [O]/[Li^+] ratios. In all

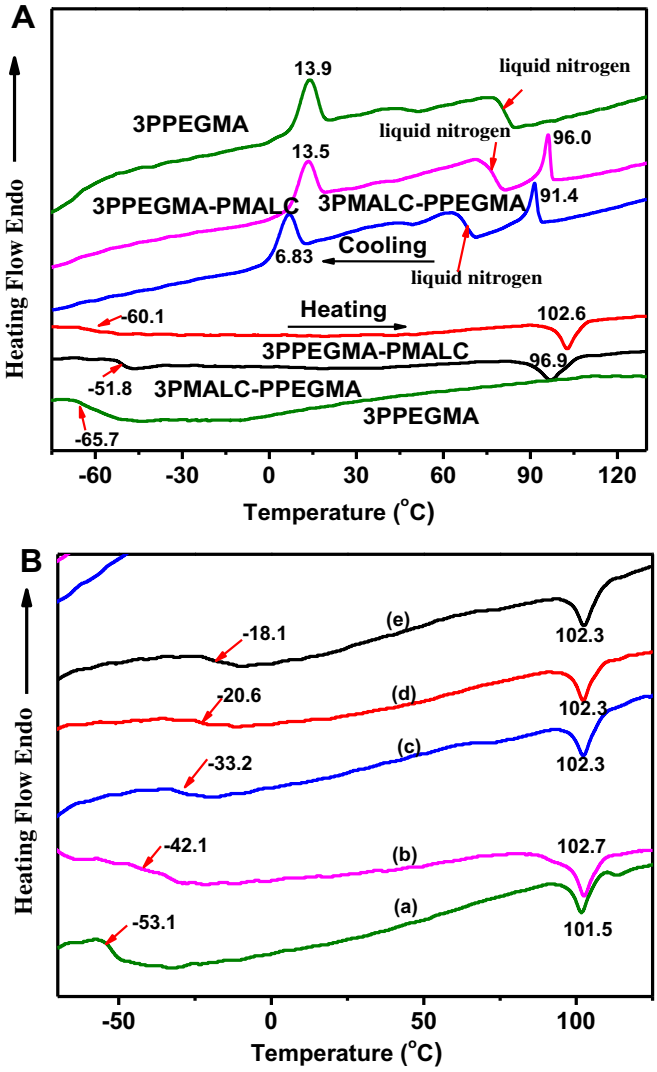

Fig. 5. DSC thermograms of (A) 3PPEGMA-PMALC, (B) its electrolytes with various [O]/[Li^+] ratios recorded under nitrogen during the second heating scans at a scan rate of 10 °C min^{-1} and [O]/[Li^+] ratios Z = (a) 30, (b) 25, (c) 20, (d) 15, and (e) 10, respectively.

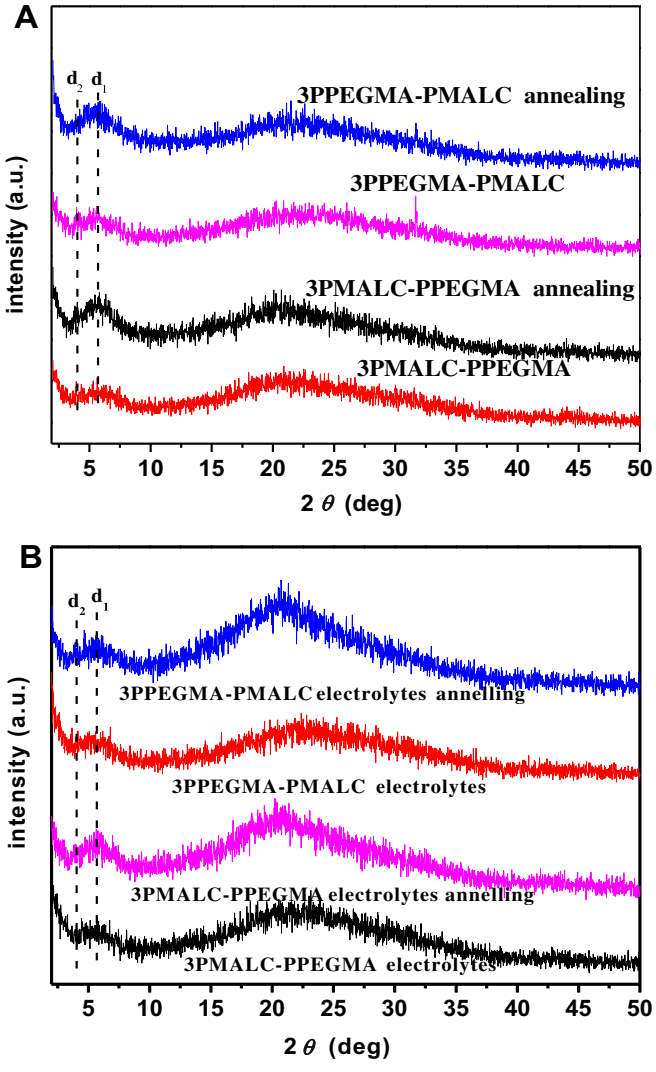

Fig. 6. XRD patterns of (A) star copolymers, (B) corresponding electrolytes ([O]/[Li^+] = 20) as-cast films and annealing from their liquid crystalline states, respectively.

cases, the salt content in the composite is kept constant related to the amount of ethylene oxide (EO) unit in the polymer. The variation of conductivity with temperatures suggests a Vogel–Tamman–Fulcher (VTF) behavior which is often observed for amorphous polymer electrolytes, suggesting that the ion mobility is coupled with the segmental motion of the polymer chain. For the 3PPEGMA-PMALC electrolyte, with a [O]/[Li^+] ratio decreasing from 30 to 20, the ionic conductivity value increases and reaches to the maximum. However, further improving the salt content results in the aggregation of salt, thus leads to a remarkable decrease in the total ionic conductivity. The conductivity data is fitted according to the VTF equation

$$\sigma T^{1/2} = A\exp\left(\frac{-E_a}{R(T-T_0)}\right) \quad (1)$$

where A is a frequency factor that is often related to the number and mobility of charge carriers, E_a is an activation energy, T_0 is the ideal transition temperature at which relaxation times become infinite and the free volume disappears, and R is the perfect gas constant, 8.314 J K^{-1} mol^{-1}. According to the literature on polyether-based polymer electrolytes, T_0 is 50 K below the glass transition temperature (T_g). [35] The VTF equation predicts that a plot of ln ($\sigma T^{1/2}$) vs. ($T - T_0$) should be linear, which is exactly observed in Fig. S7. The values of the VTF parameters for the electrolytes are listed in Table S2. The A parameter and the activation energies, Ea, in equation (1) tends to increase as the T_0 increases, exhibiting the same tendency to the literature [36,37]. Furthermore, the aggregation of salts should be responsible for the decrease in A and Ea values at the higher salt concentrations.

The ionic conductivities of the star copolymer electrolytes annealed at liquid-crystalline phase are also measured. Fig. 12 depicts the electrochemical impedance spectra of the as-cast electrolytes and annealing film at room temperature. The impedance spectra exhibit an inclined line for all samples. As for the blocking electrode used in the experiment described in Ref. [38], since there is no ion source or sink, the electrical double layer at each interface possesses infinite resistance against ion transfer, which, in the Nyquist plot of impedance spectra, would result in a straight line. The intercept of the Nyquist plot with the real axis of the impedance spectra gives the electrolyte bulk resistance (R_b). The calculated ionic conductivity values are also shown in Table 1. As expected, the ionic conductivities of the annealed electrolytes are higher than those of as-cast films, and the 3PPEGMA-PMALC shows higher conductivity than its analogous 3PMALC-PPEGMA.

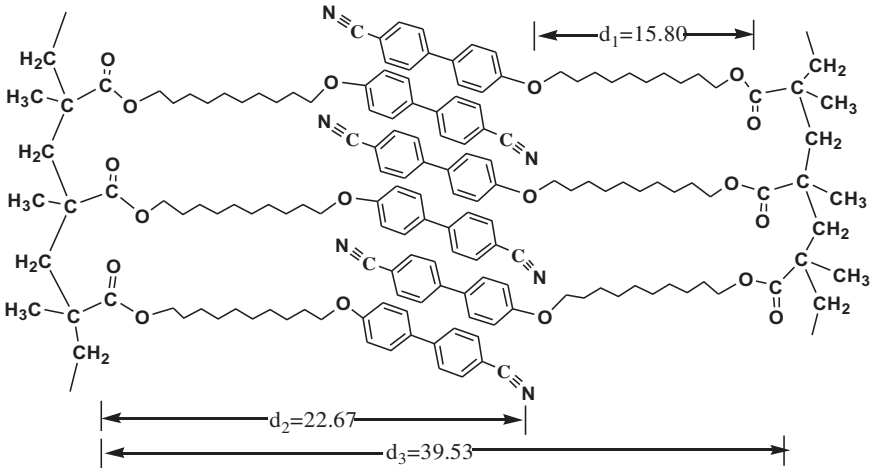

Fig. 7. Proposed bilayer packing arrangement of 3PPEGMA-PMALC with the smectogens interdigitating in antiparallel fashion.

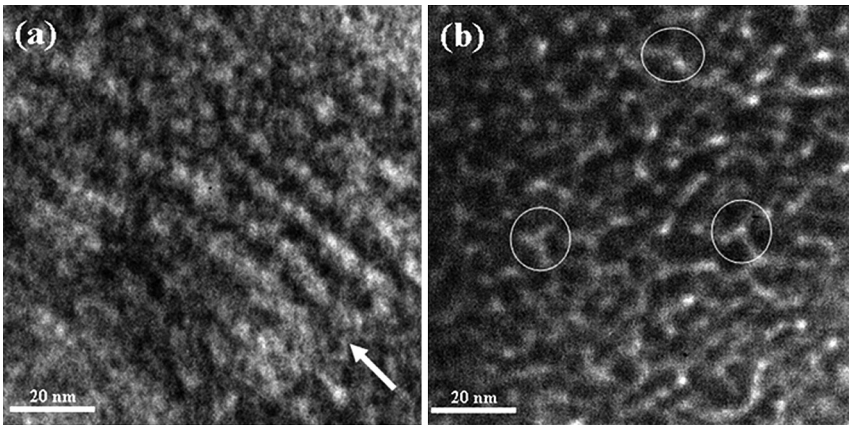

Fig. 8. TEM images of (a) 3PPEGMA-PMALC and (b) 3PMALC-PPEGMA film annealing at its liquid crystalline states (95 °C).

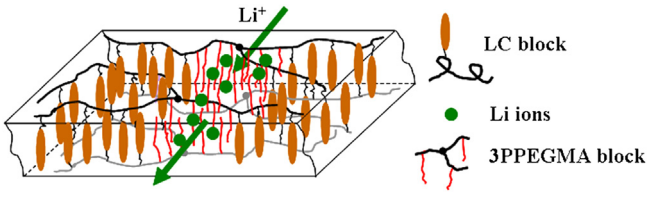

Fig. 9. Schematic depiction of the arrangement of the copolymer 3PPEGMA-PMALC annealing from the liquid crystalline state. Lithium ions are contained within the PPEGMA domain.

Particularly, electrolyte conductivity value of 3PPEGMA-PMALC is improved to 1.0×10^{-4} S cm^{-1}, even higher than that of 3PPEGMA electrolyte. The improved ionic conductivity further supports that the favorable pathway induced by cooperative self-assembly of LC group and PEGMA segment ensures more efficient and faster lithium ions transportation.

3. Conclusions

A facile strategy is developed to prepare a novel star branched amphiphilic polymethacrylate liquid crystalline block copolymers containing PEG and cyanobiphenyl side chain. The copolymer electrolytes were synthesized by adding $LiClO_4$ into 3PPEGMA-PMALC and 3PMALC-PEGMA copolymer with different ratios. The cyanobiphenyl mesogen induces all of the copolymers and electrolytes with enantiotropic liquid crystalline optical anisotropy, and nanoscale phase separation is achieved. The aligned nanostructures of the mesogen modified star branched block copolymers have

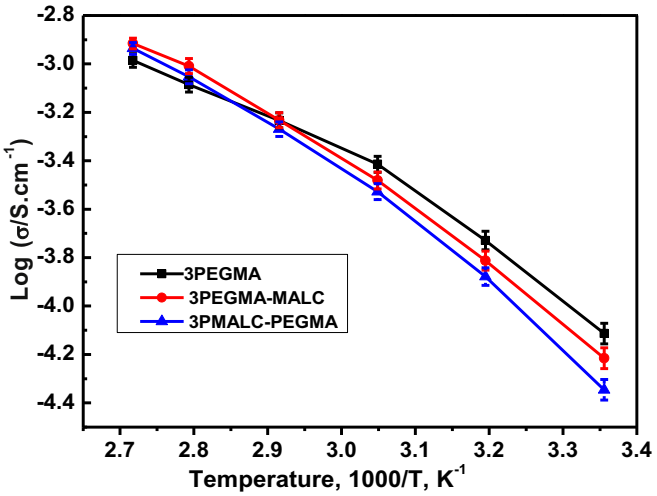

Fig. 10. Temperature dependence of ionic conductivity of 3-arm copolymers with [O]/[Li^+] = 20.

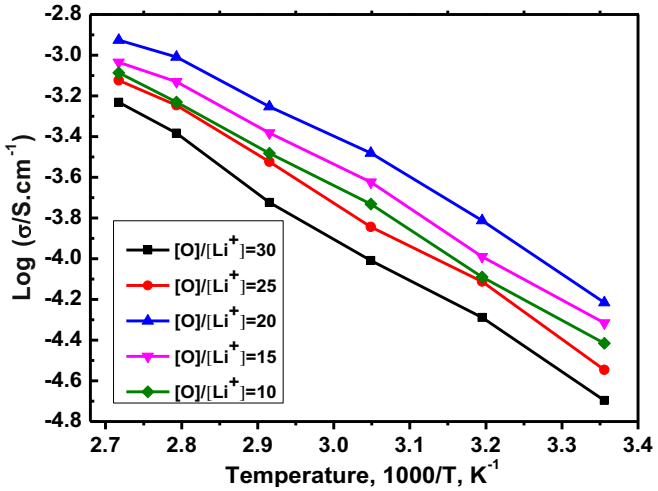

Fig. 11. Temperature dependence of ionic conductivity of 3PPEGMA-PMALC with various [O]/[Li^+] ratios.

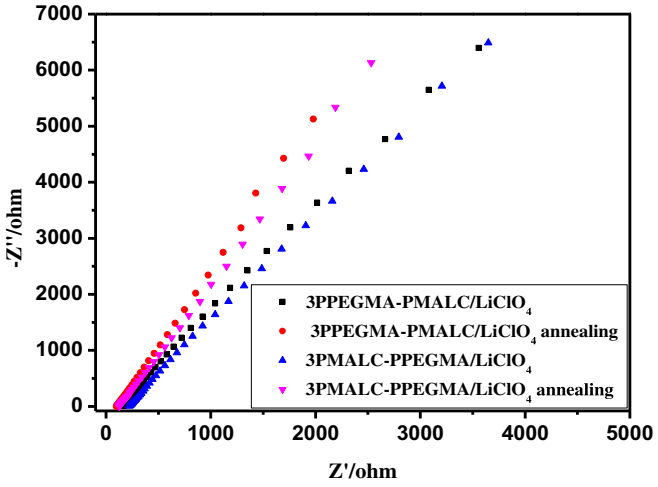

Fig. 12. AC impedance spectra of as-cast films ([O]/[Li+] = 20) and the electrolytes annealed from their liquid crystalline states recorded at room temperature.

Table 1
Ionic conductivity (at 25 °C) of as-cast films ([O]/[Li^+] = 20) and the electrolytes annealed from their liquid crystalline states.

Copolymer electrolytes		Conductivity (S cm^{-1})
3PPEGMA/$LiClO_4$	As-cast film	7.7×10^{-5}
	Annealed film	–
3PPEGMA-PMALC/$LiClO_4$	As-cast film	6.1×10^{-5}
	Annealed film	1.0×10^{-4}
3PMALC-PPEGMA/$LiClO_4$	As-cast film	4.5×10^{-5}
	Annealed film	8.1×10^{-5}

been demonstrated by cooperative assembly of hydrophobic mesogen-containing polymethacrylate groups and the amorphous hydrophilic PPEGMA nanoscale aggregation. Incorporation mesogen into star branched blocked polymers leads to significant improvement of ionic conductivity and thermal annealing from LC states can further enhance the ionic conductivity. The sequential effect of the LC segment in the copolymer electrolytes results in the morphology of copolymer electrolytes quite different. Compared with the LC segment arranged in the star copolymer interior sphere (3PMALC-PPEGMA), the one in exterior sphere (3PPEGMA-PMALC) induces more favorable ions pathway for ions transportation. The highest room temperature ionic conductivity is found to be 1.0×10^{-4} S cm^{-1} for the 3PPEGMA-PMALC/$LiClO_4$ electrolyte with [O]/[Li^+] ratio of 20 after annealing. We believe that the polymer electrolytes combining the LC group with branched, block structure should be a good candidate for all-solid-state lithium ions batteries.

Appendix A. Supplementary data

Supplementary data related to this article can be found at http://dx.doi.org/10.1016/j.jpowsour.2013.08.139.

References

[1] C.A. Vincent, B. Scrosati (Eds.), Modern Batteries, an Introduction to Electrochemical Power Sources, Butterworth-Heinemann, London, 1997.
[2] F.M. Gray, in: Solid Polymer Electrolytes, Fundamentals and Technological Applications, VCH, New York, 1991.
[3] P. Judeinstein, F. Roussel, Adv. Mater. 17 (2005) 723–727.
[4] D. Saikia, Y.H. Chen, Y.C. Pan, J. Fang, L.D. Tsai, G.T.K. Fey, H.M. Kao, J. Mater. Chem. 21 (2011) 10542–10551.
[5] N. Yoshimoto, O. Shimamura, T. Nishimura, M. Egashira, M. Nishioka, M. Morita, Electrochem. Commun. 11 (2009) 481–483.
[6] M. Patel, M. Gnanavel, A.J. Bhattacharyya, J. Mater. Chem. 21 (2011) 17419–17424.
[7] M. Higa, K. Yaguchi, R. Kitani, Electrochim. Acta 55 (2010) 1380–1384.
[8] X. Zuo, X.M. Liu, F. Cai, H. Yang, X.D. Shen, G. Liu, J. Mater. Chem. 22 (2012) 22265–22271.
[9] T. Niitani, M. Shimada, K. Kawamura, K. Dokko, Y.H. Rho, K. Kanamura, Electrochem. Solid-State Lett. 8 (2005) A385–A388.
[10] Y. Zhao, J. Soft Matter 5 (2009) 2686–2693.
[11] P.W. Majewski, M. Gopinadhan, W.S. Jang, J.L. Lutkenhaus, C.O. Osuji, J. Am. Chem. Soc. 132 (2010) 17516–17522.
[12] H.F. Yu, K. Okano, A. Shishido, T. Ikeda, K. Kamata, M. Komura, T. Iyoda, Adv. Mater. 17 (2005) 2184–2188.
[13] G. Wang, X. Tong, Y. Zhao, Macromolecules 37 (2004) 8911–8917.
[14] I. Yosuke, K. Kenji, S. Yoshimitsu, Y. Masafumi, M. Tomohiro, K. Ichiro, O. Hiroyuki, K. Takashi, Macromolecules 40 (2007) 4874–4878.
[15] Y. Zhao, B. Qi, X. Tong, Y. Zhao, Macromolecules 41 (2008) 3823–3831.
[16] G. Allegra, F. Ganazzoli, Prog. Polym. Sci. 16 (1991) 463–508.
[17] K. Inoue, Prog. Polym. Sci. 25 (2000) 453–571.
[18] G. Lapienis, Prog. Polym. Sci. 34 (2009) 852–892.
[19] T. Niitani, M. Amaike, H. Nakano, K. Dokko, K. Kanamura, J. Electrochem. Soc. 156 (2009) A577–A583.
[20] D.G. Kim, H.S. Sohn, S.K. Kim, A. Lee, J.C. Lee, J. Polym. Sci. Part A Polym. Chem. 50 (2012) 3618–3627.
[21] V. Percec, B. Barboiu, Macromolecules 28 (1995) 7970–7972.
[22] M. Kato, M. Kamigaito, M. Sawamoto, T. Higashimur, Macromolecules 28 (1996) 1721–1723.
[23] K. Min, H. Gao, K. Matyjaszewski, J. Am. Chem. Soc. 127 (2005) 3825–3830.
[24] H.F. Yu, T. Ikeda, T. Iyoda, Adv. Mater. 18 (2006) 2213–2215.
[25] H.F. Yu, A. Shishido, J. Li, K. Kamata, T. Iyoda, T. Ikeda, J. Mater. Chem. 17 (2007) 3485–3488.
[26] K. Yao, Y.W. Chen, L. Chen, F. Li, X. Li, X. Ren, H.M. Wang, T. Liu, Macromolecules 44 (2011) 2698–2706.
[27] W.H. Hou, C.Y. Chen, C.C. Wang, Polymer 44 (2003) 2983–2991.
[28] Y.H. Liang, C.C. Wang, C.Y. Chen, Eur. Polym. J. 44 (2008) 2376–2384.
[29] H. Y Wu, D. Saikia, C.P. Lin, F.S. Wu, G.T.K. Fey, H.M. Kao, Polymer 51 (2010) 4351–4361.
[30] J. Wu, T.S. Haddad, P.T. Mather, Macromolecules 42 (2009) 1142–1152.
[31] B.D. Olsen, X. Gu, A. Hexemer, E. Gann, R.A. Segalman, Macromolecules 43 (2010) 6531–6534.
[32] C. Park, J. Yoon, E.L. Thomas, Polymer 44 (2003) 6725–6760.
[33] Z.H. Shi, D.Z. Chen, H.J. Lu, B. Wu, J. Ma, R.S. Cheng, J.L. Fang, X.F. Chen, Soft Matter 8 (2012) 6174–6184.
[34] K. Kishimoto, T. Suzawa, T. Yokota, T. Mukai, H. Ohno, T. Kato, J. Am. Chem. Soc. 127 (2005) 15618–15623.
[35] G. Adam, J.H. Gibbs, J. Chem. Phys. 43 (1965) 139–146.
[36] M.A.S.A. Samir, F. Alloin, J.Y. Sanchez, A. Dufresne, Macromolecules 37 (2004) 4839–4844.
[37] N. Binesh, S.V. Bhat, J. Polym. Sci. Part B Polym. Phys. 36 (1998) 1201–1209.
[38] J.R. Macdonald, Impedance Spectroscopy, Wiley, New York, 1987.